THE JOURNAL OF BIOLOGICAL CHEMISTRY
Vol. 277, No. 12, Issue of March 22, pp. 9661–9667, 2002

Printed in U.S.A.

Role of Nucleotidyl Transferase Motif V in Strand Joining by *Chlorella* Virus DNA Ligase*

Received for publication, November 5, 2001
Published, JBC Papers in Press, December 20, 2001, DOI 10.1074/jbc.M110613200

Verl Sriskanda and Stewart Shuman‡

From the Molecular Biology Program, Sloan-Kettering Institute, New York, New York 10021

ATP-dependent DNA ligases, NAD$^+$-dependent DNA ligases, and GTP-dependent RNA capping enzymes are members of a covalent nucleotidyl transferase superfamily defined by a common fold and a set of conserved peptide motifs. Here we examined the role of nucleotidyl transferase motif V (^{184}LLKMKQFKDAEAT^{196}) in the nick joining reaction of *Chlorella* virus DNA ligase, an exemplary ATP-dependent enzyme. We found that alanine substitutions at Lys^{186}, Lys^{188}, Asp^{192}, and Glu^{194} reduced ligase specific activity by at least an order of magnitude, whereas substitutions at Lys^{191} and Thr^{196} were benign. The K186A, D192A, and E194A changes had no effect on the rate of single-turnover nick joining by preformed ligase-adenylate but affected subsequent rounds of nick joining at the ligase adenylation step. Conservative substitutions K186R, D192E, and E194D partially restored activity, whereas K186Q, D192N, and E194Q substitutions did not. Alanine mutation of Lys^{188} elicited distinctive catalytic defects, whereby single-turnover nick joining by K188A-adenylate was slowed by an order of magnitude, and high levels of the DNA-adenylate intermediate accumulated. The rate of phosphodiester bond formation at a pre-adenylated nick (step 3 of the ligation pathway) was slowed by the K188A change. Replacement of Lys^{188} by arginine reversed the step 3 arrest, whereas glutamine substitution was ineffective. Gel-shift analysis showed that the Lys^{188} mutants bound stably to DNA-adenylate. We infer that Lys^{188} is involved in the chemical step of phosphodiester bond formation.

DNA ligases and RNA capping enzymes comprise distinct branches of a covalent nucleotidyl transferase superfamily defined by a common protein fold (1–6). Ligases and capping enzymes catalyze two chemically similar partial reactions entailing the transformation of an α-β phosphoanhydride bond (in ATP, NAD$^+$, or GTP) into a phosphoamide (an enzyme-lysyl-AMP or -lysyl-GMP intermediate) and then back into a phosphoanhydride (AppDNA or GpppRNA) (7, 8). Whereas the guanylyltransferase reaction is complete after formation of GpppRNA, the DNA ligases catalyze a third step in which the phosphoanhydride is converted into a phosphodiester by nucleophilic attack of a DNA 3′ OH on the DNA 5′ PO_4 of AppDNA. The peptide motifs that form the nucleotide binding pocket are conserved in the tertiary structures of DNA ligases and capping enzymes (2–6), which raises the question of whether specific functional groups are put to similar uses during catalysis of ligation and capping. Other key questions pertain to the third step that is unique to DNA ligases. Are the residues involved in catalysis of steps 1 and 2 also exploited by DNA ligases in catalysis of the strand sealing step? Do ligases have additional catalytic residues that function specifically during step 3?

To address these issues, we have initiated comparative structure-function analyses of exemplary DNA ligases and RNA guanylyltransferases (9–12). We are studying the mechanism of ATP-dependent DNA ligase using *Chlorella* virus ligase as a model. The 298-amino acid *Chlorella* virus enzyme is the smallest eukaryotic ATP-dependent ligase known (13), and the atomic structure of the ligase-adenylate catalytic intermediate has been solved by x-ray crystallography (4). The *Chlorella* virus ligase consists of a 188-amino acid N-terminal domain (domain 1) and a 110-amino acid C-terminal domain (domain 2). Within the N-terminal domain is an adenylate binding pocket composed of five motifs (I, III, IIIa, IV, and V) that define the ligase/capping enzyme superfamily (Fig. 1). The C-terminal domain adopts an oligomer-binding fold, consisting of a five-stranded antiparallel β barrel and an α helix. The oligomer-binding fold domain includes at its C terminus nucleotidyl transferase motif VI, which is conserved in capping enzymes and ATP-dependent DNA ligases. Our aim is to delineate structure-activity relationships for the *Chlorella* virus ligase that will illuminate the general mechanism of covalent nucleotidyl transfer and provide specific insights into the basis for DNA recognition and step 3 chemistry.

Motif I (^{27}K*X*DG*X*R) contains the lysine nucleophile to which AMP becomes covalently linked in the first step of the *Chlorella* virus ligase reaction (4). Mutation of Lys^{27} to alanine abolishes the overall nick joining reaction by preventing formation of the ligase-AMP intermediate (9). Of course, this mutation also precludes the second step of the pathway, which entails the transfer of AMP from ligase-adenylate to 5′ phosphate of the nick to form an activated DNA-adenylate intermediate. Lys^{27} is not essential for catalysis of phosphodiester bond formation on a preformed nicked DNA-adenylate substrate (step 3), although the K27A mutation does slow the rate of step 3 by an order of magnitude (9, 10). The motif I aspartate (Asp^{29}) is not important for formation of ligase-adenylate but is essential for the subsequent steps of the pathway, especially step 2 (4, 9). The rate of single-turnover nick joining (steps 2 and 3) by the D29A ligase-AMP intermediate is slower, by a factor of 6000, than the rate of the wild-type ligase-adenylate (14), whereas in the isolated step 3 reaction, the D29A mutation elicited a 60-fold rate decrement (15). Asparagine substitution for Asp^{29} reduced the rate of single-turnover nick ligation to 2% of the wild-type rate (9) but had no discernible impact on the rate of step 3 (15). Thus, the carboxylate moiety is critical for catalysis of step 2, but an amide suffices during step 3. These results

* This work was supported by National Institutes of Health Grant GM63611. The costs of publication of this article were defrayed in part by the payment of page charges. This article must therefore be hereby marked "*advertisement*" in accordance with 18 U.S.C. Section 1734 solely to indicate this fact.
‡ To whom correspondence should be addressed. E-mail: s-shuman@ski.mskcc.org.

provided initial evidence for nonequivalence of the active sites during the three chemical steps of the ligation reaction.

By extending the alanine scanning and conservative mutational analysis to other side chains in the nucleotidyl transferase motifs, we found that Arg^{32} in motif I, Asp^{65} and Glu^{67} in motif III, Phe^{98} in motif IIIa, and Glu^{161} in motif IV are essential for overall nick joining but play distinct roles at different component steps (4, 9, 15). Arg^{32} is required for steps 1 and 3. Arg^{32} contacts the ribose sugar of adenosine and forms a salt bridge with Asp^{65}, which is also required for steps 1 and 3. Conservative mutational effects indicate that the salt bridge is essential, and we have proposed that the role of Asp^{65} is to correctly position Arg^{32} in the active site (15). The motif III Glu^{67} carboxylate is essential for steps 1 and 3; the equivalent motif III glutamate of T7 ligase contacts the adenosine ribose in the T7 ligase-ATP crystal (3). Based on mutational data and comparison of the *Chlorella* virus and T7 ligase crystal structures, we have proposed that the conformation of the adenosine nucleoside (and the contacts of the ribose to the enzyme) are remodeled at sequential steps of the ligase pathway (4). Replacement of motif IIIa residue Phe^{98} by alanine selectively impairs the step 1 reaction with ATP to form ligase-adenylate but has no impact on nick joining by preformed F98A-adenylate intermediate (15). Phe^{98} forms a π stack on the adenine base of the nucleotide, and activity can be restored partially by introduction of a leucine in place of the aromatic ring. The motif IV Glu^{161} side chain is essential for reactions 1 and 3, but structure-activity relationships suggest that Glu^{161} acts differently in step 1 *versus* step 3. Whereas a carboxylate at position 161 is absolutely essential for step 1 (consistent with a proposed role of Glu^{161} in metal binding), its role in phosphodiester formation can be fulfilled by glutamine with only an 8-fold decrement in the step 3 reaction rate (15). Motif VI at the C terminus of *Chlorella* virus ligase is uniquely required for step 1 of the nick joining reaction (10).

In the present study, we focused on the catalytic role of nucleotidyl transferase motif V (Fig. 1*A*). Motif V (^{184}LLKMKQFKDAEAT^{196}) serves as the bridging segment between domains 1 and 2 of *Chlorella* virus ligase. Motif V consists of two β strands, one in domain 1 and a second in domain 2, with a short interstrand linker (Fig. 1*A*). Comparison of the T7 and *Chlorella* virus DNA ligase structures, as well as the *Chlorella* virus guanylyltransferase structure, shows that the linker is a flexion point for movements of domain 2 relative to domain 1 that are believed to be coordinated with the substrate binding and product release steps of the ligation pathway (2–4). It is proposed that catalysis of nucleotidyl transfer step 1 is facilitated by closure of the oligomer-binding fold domain over the nucleotide binding pocket such that motif VI (located at the C terminus of the oligomer-binding fold) makes direct contact with the β and γ phosphates and reorients the pyrophosphate leaving group so that it is apical to the attacking lysine (2). Once the proper orientation is attained, the lysyl-AMP intermediate is formed, and pyrophosphate is expelled. The breaking of the α-β phosphoanhydride bond would release the tether of motif VI to the nucleotidyl transferase domain and trigger the adoption of a wide open domain conformation that permits the binding of the nicked DNA substrate immediately above the AMP phosphate on the surface of the nucleotidyl transferase domain (4).

Here we performed alanine scanning and conservative mutagenesis of six individual amino acids within motif V. The findings highlight contributions of Lys^{186}, Asp^{192}, and Glu^{194} to nick joining and specifically to the ligase-adenylation reaction (step 1). Lys^{188} is implicated as a step 3 catalyst because mutations of Lys^{188} result in substantial accumulation of the normally evanescent DNA-adenylate intermediate and a defect in strand joining at a pre-adenylated nick. The findings are discussed in light of available mutational data for motif V of yeast RNA capping enzyme and *Escherichia coli* NAD^+-dependent DNA ligase (11, 12).

EXPERIMENTAL PROCEDURES

Ligase Mutants—Missense mutations of motif V were introduced into the pET-ChVLig or pET-ChVLigCΔ5 expression plasmids as described previously (9, 10). The entire gene was sequenced in every case to confirm the desired mutation and exclude the acquisition of unwanted changes during PCR amplification and cloning. The expression plasmids were transformed into *E. coli* BL21(DE3). Mutant and wild-type ligases were purified from the soluble lysates of isopropyl-1-thio-β-D-galactopyranoside-induced BL21(DE3) cells by Ni-agarose and phosphocellulose chromatography as described previously (9). The protein concentrations of the phosphocellulose enzyme preparations were determined using the Bio-Rad dye reagent with bovine serum albumin as a standard. SDS-PAGE analysis of the motif V mutants of full-length *Chlorella* virus ligase is shown in Fig. 2; analysis of the CΔ5 mutants in shown in Fig. 6*A*.

Assay of Nick Joining—Reaction mixtures (20 μl) containing 50 mM Tris-HCl (pH 7.5), 5 mM DTT,[1] 10 mM $MgCl_2$, 1 mM ATP, 500 fmol of 5′ ^{32}P-labeled nicked duplex DNA substrate, and aliquots of serial 2-fold dilutions of wild-type or mutant ligases were incubated at 22 °C for 10 min. The products were resolved by denaturing PAGE, and the extents of ligation were determined by scanning the gel using a FUJIX BAS2000 phosphorimaging system. The specific activities of wild-type and mutant ligases were determined from the slopes of the titration curves in the linear range of enzyme dependence.

Ligation at a Pre-adenylated Nick—The nicked DNA-adenylate substrate is shown in Fig. 6*B*. The 5′ adenylated ^{32}P-labeled 18-mer strand was synthesized and gel-purified as described previously (16). The DNA-adenylate ligation reaction mixtures (20 μl) contained 50 mM Tris-HCl (pH 7.5), 5 mM DTT, 5 mM $MgCl_2$, 200 fmol of nicked DNA-adenylate substrate, and "wild-type" CΔ5 (WT-CΔ5) or mutant CΔ5 proteins as specified. The mixtures were incubated for 30 min at 22 °C. The products were resolved by denaturing PAGE, and the extents of ligation were determined by scanning the gel with a phosphorimaging system. For kinetic analysis, reaction mixtures containing (per 20 μl) 200 fmol of nicked DNA-adenylate substrate and other components as specified above were incubated at 22 °C. The sealing reactions were initiated by adding enzyme. Aliquots (20 μl) were withdrawn at the times specified in the figures and quenched immediately with EDTA and formamide (9).

Binding of CΔ5 Ligase to DNA-adenylate—Reaction mixtures (20 μl) containing 50 mM Tris-HCl (pH 7.5), 5 mM DTT, 200 fmol of nicked DNA-adenylate, and 4 pmol of WT-CΔ5 or CΔ5 mutants as specified were incubated for 10 min at 22 °C. Glycerol was added to 5%, and the samples were analyzed by electrophoresis (for 2 h at 70 V) through a native 6% polyacrylamide gel containing 90 mM Tris borate, 2.5 mM EDTA (9). Free AppDNA and ligase-DNA complexes of retarded mobility were visualized by autoradiography of the dried gel.

RESULTS

Effects of Alanine Substitutions in Motif V—An initial test of the function of the Lys^{186}, Lys^{188}, Lys^{191}, Asp^{192}, Glu^{194}, and Thr^{196} side chains of motifs V (Fig. 1*A*) was performed by replacing them individually by alanine and then scoring the ability of the recombinant mutated enzymes (Fig. 2) to seal a nicked duplex DNA substrate *in vitro*. The specific activities of the K186A and K188A proteins were 7 and 2% of the wild-type ligase activity, respectively (4). The D192A and E194A proteins were 3% as active as wild-type ligase. In contrast, K191A and T196A retained 54 and 85% of the wild-type specific activity (Fig. 1*B*). We have imposed a 5-fold activity decrement as the criterion of significance for the effects of alanine substitution. Residues are deemed "important" when alanine substitution reduces specific activity to 6–20% of the wild-type value. Our operational definition of an "essential" residue is one at which alanine substitution reduces specific activity to ≤5% of the wild-type activity. By these criteria, Lys^{188}, Asp^{192}, and Glu^{194}

[1] The abbreviations used are: DTT, dithiothreitol; WT, wild type; ChV, *Chlorella* virus.

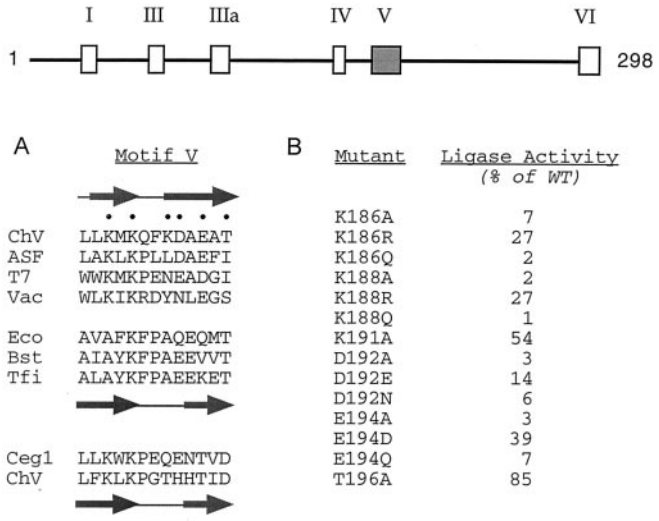

FIG. 1. **Mutational analysis of nucleotidyl transferase motif V.** The 298-amino acid *Chlorella* virus DNA ligase polypeptide is depicted as a *straight line* with the positions of conserved motifs I, III, IIIa, IV, V, and VI denoted by *boxes*. *A*, the sequence of motif V of *Chlorella* virus ligase (*ChV*) is aligned with the corresponding motif V sequences of the ATP-dependent DNA ligases of African swine fever virus (*ASF*), bacteriophage T7 (*T7*), and vaccinia virus (*Vac*); the NAD^+-dependent DNA ligase of *E. coli* (*Eco*), *Bacillus stearothermophilus* (*Bst*), and *Thermus filiformis* (*Tfi*); and the capping enzymes of *S. cerevisiae* (*Ceg1*) and *Chlorella* virus. The secondary structure elements of the ChV and *T. filiformis* ligases and the ChV capping enzyme are shown *above* or *below* the respective sequences with β strands indicated by *arrows*. Amino acid residues of ChV ligase that were targeted for mutagenesis in the present study are denoted by *dots*. *B*, the specific activities of WT and mutant ligases in nick joining were determined from the slopes of the titration curves in the linear range of enzyme dependence. The activity values for the mutant enzymes were normalized to the WT specific activity (defined as 100%).

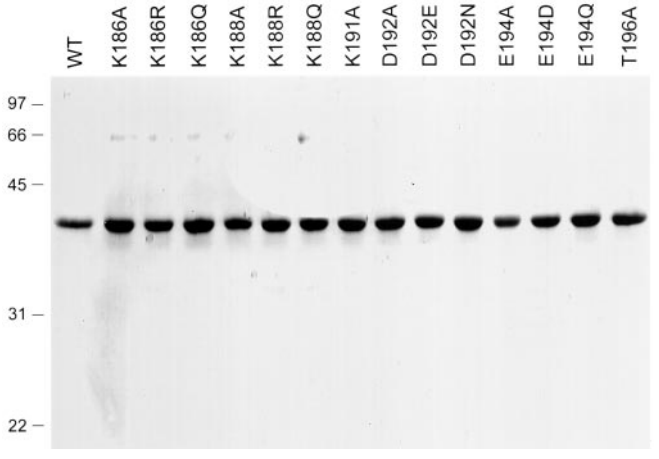

FIG. 2. **Protein purification.** Aliquots (2 μg) of the phosphocellulose fractions of full-length wild-type ligase and the indicated mutant proteins were analyzed by SDS-PAGE. Polypeptides were visualized by staining the gel with Coomassie Brilliant Blue dye. The positions and sizes (in kDa) of marker proteins are indicated on the *left*.

are essential for the overall ligation reaction, and Lys^{186} is important. Lys^{191} and Thr^{196} were deemed unimportant and were not subjected to further analysis.

Nick joining by the wild-type, K186A, K188A, D192A, and E194A proteins was assayed under single-turnover conditions, *i.e.* in the absence of added ATP. The linear dependence of the extent of nick joining on the amount of input wild-type ligase suggested that 15% of the enzyme molecules in the preparation contained covalently bound AMP (Fig. 3*A*). The titration profiles of the K186A, K188A, D192A, and E194A proteins were similar to that of wild-type ligase, indicating that ligase-adenylate comprised 8–14% of the mutant enzyme preparations. We then performed a kinetic analysis of single-turnover strand joining by wild-type and mutant ligases present in 12-fold molar excess over the nicked DNA substrate. The reactions proceeded to similar end points with ~80–90% of the input substrate being sealed (Fig. 3*B*). Wild-type ligase attained 78% of the end point in 5 s; from this datum, we calculated an apparent rate constant of 0.3 s^{-1}. The rates of approach to the end point by the K186A, D192A, and E194A enzymes were nearly identical to the wild-type rate. Because K186A, D192A, and E194A were as active as the wild-type ligase in nick joining catalyzed by preformed ligase-adenylate (reflecting steps 2 and 3 of the ligase pathway) but were only 3–7% as active under steady-state conditions, we suspected that these three mutants were specifically defective in the step 1 reaction of ligase with free ATP to form ligase-adenylate.

This point was underscored by kinetic analysis of the nick joining reaction in the presence of 12.5 nM nicked DNA, 20 nM ligase (corresponding to ~2–3 nM ligase-AMP), and 1 mM ATP (Fig. 4*A*). Wild-type ligase joined >80% of the input substrate and attained its end point in 15 s; the approach to the end point was smooth. In contrast, the K186A, D192A, and E194A mutants displayed biphasic kinetics characterized by an initial burst of nick joining in 10 s followed by a slow phase of approach to the end point from 15 s to 2 min (K186A and D192A) or 6 min (E194A). The amplitudes of the bursts (90–140 fmol of nicks sealed) corresponded closely to the amounts of ligase-adenylate included in the individual reaction mixtures. Therefore we surmise that the burst phase of the K186A, D192A, and E194A reactions reflected the rapid single-turnover joining of nicks by preformed ligase-AMP, and the second slow phase reflected the effects of the mutations on the rate of the ligase-adenylation step of the reaction pathway. A comparison of the extents of covalent ligase-[^{32}P]AMP adduct formation during a 5-min reaction of wild-type and mutant ligases with [α-^{32}P]ATP *in vitro* verified that the K186A, D192A, and E194A mutants were impaired to varying degrees in the ligase adenylation step (Fig. 4*B*). The yields of ligase-[^{32}P]AMP relative to wild-type were 56% for K186A, 21% for D192A, and 11% for E194A.

The K188A Mutation Elicits a Step 3 Arrest—An instructive finding from the kinetic analysis was that the rate of single-turnover nick joining by the adenylated K188A ligase was slowed significantly compared with wild-type ligase and the other motif V mutants (Fig. 3*B*). The reaction of K188A attained an end point in 2–4 min, and the apparent rate constant of 0.02 s^{-1} was ~7% of the wild-type rate. Moreover, K188A did not display an initial rapid burst of nick joining in the presence of ATP (Fig. 4*A*). Rather the K188A reaction resulted in a steady accumulation of ligated product, reaching its end point after 8 min. This kinetic behavior suggested that the K188A reaction was defective at a step downstream of ligase adenylation.

The nature of the defect was clarified by comparative analysis of the reaction products of wild-type and K188A ligase-adenylate with nicked DNA under single-turnover conditions (enzyme excess, no added ATP). Wild-type ligase catalyzed rapid nick joining with no detectable DNA-adenylate formation; the reaction reached its end point in 15 s (Fig. 5). In contrast, K188A catalyzed a rapid burst of DNA-adenylate formation, with ~75% of the input 5′ phosphate strand at the nick becoming adenylated in 15 s (Fig. 5). Ligated product accumulated steadily from 15 to 60 s concomitant with a decline in DNA-adenylate. These results indicate that the K188A mutation selectively impairs the third step of the ligation path-

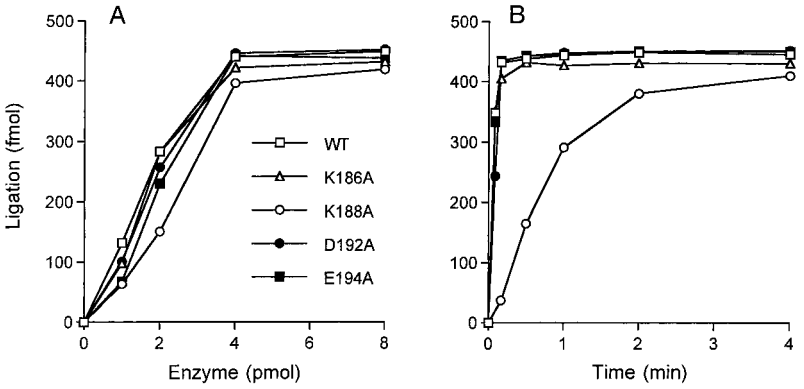

FIG. 3. **Effects of motif V mutations on single-turnover nick ligation.** *A*, ligase titration. Reaction mixtures (20 μl) containing 50 mM Tris-HCl (pH 7.5), 5 mM DTT, 10 mM $MgCl_2$, 500 fmol of 5′ ^{32}P-labeled nicked duplex DNA substrate, and WT or mutant ligases as specified were incubated at 22 °C for 10 min. The extent of strand joining is plotted as a function of input ligase. *B*, kinetics. Reaction mixtures containing (per 20 μl) 50 mM Tris-HCl (pH 7.5), 5 mM DTT, 10 mM $MgCl_2$, 500 fmol of 5′ ^{32}P-labeled nicked duplex DNA substrate, and 6 pmol of WT or mutant ligases were incubated at 22 °C. The reactions were initiated by the addition of ligase. Aliquots (20 μl) were withdrawn at the times specified and quenched immediately with EDTA and formamide. The extent of ligation is plotted as a function of time.

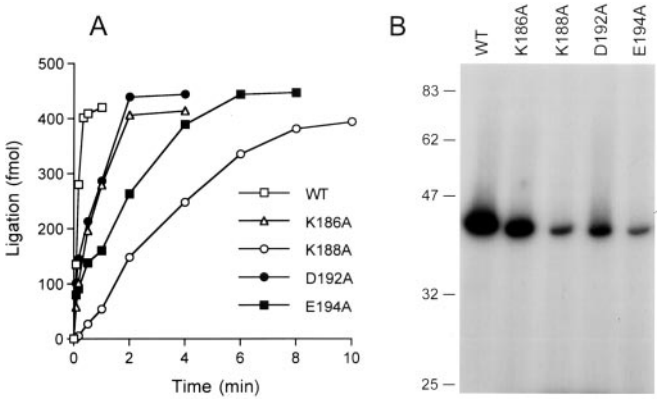

FIG. 4. **Kinetics of nick ligation in the presence of ATP.** *A*, reaction mixtures containing (per 20 μl) 50 mM Tris-HCl (pH 7.5), 5 mM DTT, 10 mM $MgCl_2$, 500 fmol of 5′ ^{32}P-labeled nicked duplex DNA substrate, and 1 pmol of WT or mutant ligases were incubated at 22 °C. Aliquots (20 μl) were withdrawn at the times specified and quenched immediately. Ligation is plotted as a function of time. *B*, reaction mixtures (20 μl) containing 50 mM Tris-HCl (pH 8.0), 5 mM DTT, 5 mM $MgCl_2$, 5 μM [α-^{32}P]ATP, and 4 pmol of the indicated ligase preparations were incubated for 5 min at 22 °C. Reactions were quenched by adding SDS to 1%. The reaction products were resolved by SDS-PAGE. An autoradiogram of the dried gel is shown.

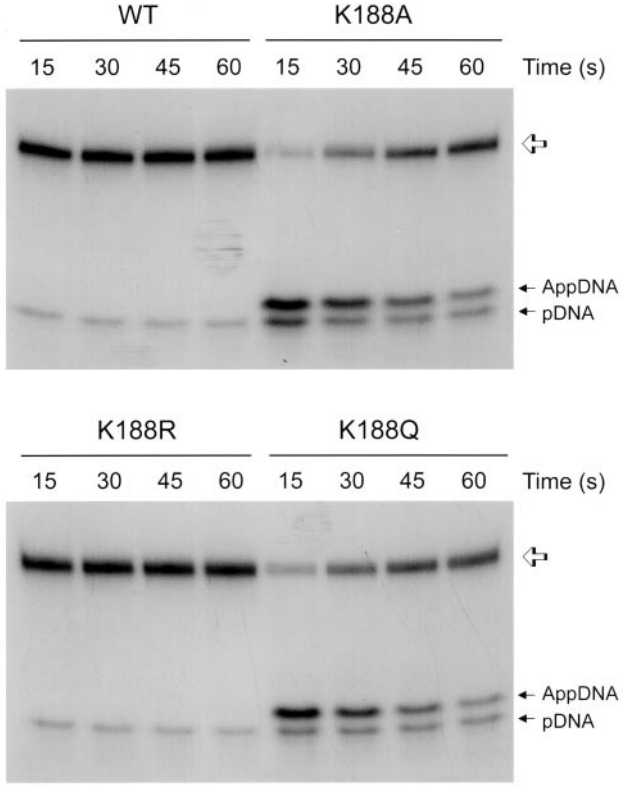

FIG. 5. **Lys^{188} mutants display a step 3 arrest with accumulation of DNA-adenylate.** Single-turnover ligation reaction mixtures containing (per 20 μl) 500 fmol of 5′ ^{32}P-labeled nicked duplex DNA substrate and 6 pmol of WT, K188A, K188R, or K188Q ligase were incubated at 22 °C. Aliquots (20 μl) were withdrawn at 15, 30, 45, and 60 s and quenched immediately with EDTA and formamide. The reaction products were resolved by denaturing PAGE and visualized by autoradiography. The positions of the 5′ ^{32}P-labeled 18-mer substrate (*pDNA*) and the DNA-adenylate intermediate (*AppDNA*) are indicated by *thin arrows* on the right. The 36-mer ligation product is indicated by a *thick arrow*.

way (the attack of the 3′ OH on DNA-adenylate to form a phosphodiester) relative to step 2 (transfer of AMP from ligase-adenylate to the nick) to the point that step 3 is rendered rate-limiting during the single-turnover nick joining reaction. The K188A mutation also affected the ligase adenylation step such that the extent of ligase-[^{32}P]AMP adduct formed *in vitro* by K188A was 13% of the wild-type value (Fig. 4*B*).

Effects of Conservative Motif V Mutations on Nick Joining—To evaluate the roles of charge, hydrogen bonding potential, and steric constraints in the functions of the motif V residues, we replaced Lys^{186} and Lys^{188} by arginine and glutamine. Asp^{192} was substituted conservatively by asparagine and glutamate, and Glu^{184} was replaced by glutamine and aspartate. The recombinant mutant ligases were purified from soluble bacterial extracts by Ni-agarose and phosphocellulose column chromatography (Fig. 2). The specific activity of each mutant was determined under steady-state conditions by protein titration and normalized to the specific activity of wild-type ligase; the results are summarized in Fig. 1*B*. We found that the defect imposed by the K186A mutation (7% of wild-type activity) was partially ameliorated by arginine (27% activity) but not at all by glutamine (2% activity). The more severe defect of the K188A mutation (2% activity) was rescued substantially by arginine (27%), whereas glutamine had no salutary effect (1% activity). Replacing Asp^{192} with glutamate elicited a partial gain of function (14% activity) compared with D192A (2%), but the isosteric amide of asparagine did not revive activity. An aspartic acid at position Glu^{194} enhanced activity >10-fold (to 39% of wild-type) compared with E194A (3%), but glutamine was of little help. We conclude that (i) a

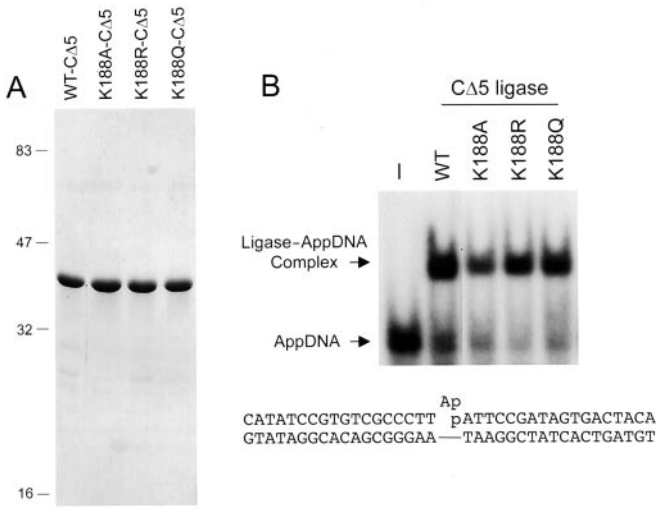

FIG. 6. **Lys^{188} mutations of CΔ5 ligase.** *A*, purification. Aliquots (4 μg) of the phosphocellulose fractions of WT-CΔ5 and the indicated mutant CΔ5 proteins were analyzed by SDS-PAGE. Polypeptides were visualized by staining the gel with Coomassie Brilliant Blue dye. *B*, binding of the indicated CΔ5 ligases to the nicked DNA-adenylate substrate (shown at *bottom*) was assayed as described under "Experimental Procedures." An autoradiogram of the native gel is shown. The positions of free AppDNA and the ligase-AppDNA complex are indicated by *arrows*.

positive charge is important at position 186 and essential at position 188; (ii) carboxylates are essential at positions 192 and 194; and (iii) conservative substitutions that preserved the charge but alter the distance from the main chain to the essential functional group elicit modest reductions in activity but are not catastrophic.

We examined the effects of the K188Q and K188R mutations on single-turnover nick joining. K188Q displayed the same step 3 block as K188A, evinced by the accumulation of high levels of the DNA-adenylate intermediate at 15 s and its decay over 15–60 s as ligated product was formed (Fig. 5). Introduction of arginine alleviated the step 3 block such that no DNA-adenylate was detected and the reaction was complete at 15 s (Fig. 5). These results underscore the requirement for a basic side chain at position 188 in catalysis of phosphodiester bond formation.

Effects of Lys^{188} Mutations on Phosphodiester Formation at a Pre-adenylated Nick—Step 3 of the *Chlorella* virus ligase reaction can be studied in isolation by assaying the ability of wild-type and mutant enzymes to seal a pre-adenylated nicked duplex DNA (9) (Fig. 6). Ligase reacts with this substrate in the absence of ATP to catalyze phosphodiester bond formation. Defects in step 3 catalysis can be gauged only qualitatively by assays of full-length wild-type and mutant ligases. A quantitative analysis of mutational effects on step 3 requires that the mutations of interest be transferred into the CΔ5 deletion variant of *Chlorella* virus ligase. The rate of ligation of a pre-adenylated nick by CΔ5 (which lacks motif VI) is 16-fold faster than the wild-type rate (10). We proposed that the loss of motif VI overcomes a rate-limiting conformational step that is unique to the reaction of ligase with an *exogenous* nicked DNA-adenylate substrate (10). The key issue for the structure-function analysis is that mutational effects on step 3 catalysis can be detected and quantitated with at least 10-fold higher sensitivity in the CΔ5 background than they can in the context of the full-sized ligase.

We introduced the K188A, K188R, and K188Q changes into the CΔ5 protein. The WT-CΔ5 and the three mutants were purified from soluble bacterial extracts by Ni-agarose and phosphocellulose chromatography (Fig. 6*A*). The extent of sealing of the nicked-DNA adenylate during a 30 min reaction was proportional to the amount of input WT-CΔ5; 75% of the input substrate was ligated at saturating levels of enzyme (Fig. 7A). The K188R-CΔ5, K188Q-CΔ5, and K188A-CΔ5 enzymes attained saturation at 70–75% strand joining. Although the mutant CΔ5 titration curves were shifted slightly to the right, the slopes of the curves in the linear range were similar to that of WT-CΔ5. A kinetic analysis of the step 3 reaction in enzyme excess is shown in Fig. 7*B*. The WT-CΔ5 reaction attained 68% of the end point value at 10 s, from which we estimated a rate constant of ~7 min^{-1}. The rate of K188R-CΔ5 was as fast or faster than that of WT-CΔ5 such that the reaction end point was reached within 10 s. K188Q-CΔ5 and K188A-CΔ5 reacted slowly with apparent rate constants of 0.9 min^{-1}. We surmise that Lys^{188} accelerates the rate of the isolated step 3 reaction by about 8-fold, and an arginine fully suffices for performance of this step.

Effects of Lys^{188} Mutations on Binding of CΔ5 Ligase to DNA-adenylate—A mixture of 200 nM WT-CΔ5 with 10 nM nicked DNA-adenylate in the absence of a divalent cation (omission of which precludes phosphodiester formation) resulted in the formation of a discrete ligase-AppDNA complex that migrated more slowly than free DNA-adenylate during native gel electrophoresis (Fig. 6*B*). The majority of the input DNA-adenylate was bound to the ligase under these conditions. We found that CΔ5 mutants K188A, K188R, and K188Q bound to nicked DNA-adenylate (Fig. 6*B*). These results engender an interpretation of the deleterious effects of the K188A and K188Q mutations on step 3 under single-turnover conditions as indicative of a role for Lys^{188} in the chemical step of phosphodiester bond formation.

Ligase Activity in Vivo—Budding yeast provides a surrogate genetic assay for scoring mutational effects on *Chlorella* virus DNA ligase function *in vivo* (12). Viability of a *Saccharomyces cerevisiae cdc9*Δ strain deleted at the chromosomal locus encoding the essential Cdc9 DNA ligase is contingent on maintenance of an extrachromosomal *CDC9* gene on a *CEN URA3* plasmid. Hence, *cdc9*Δ cells cannot grow on medium containing 5-fluoroorotic acid, a drug that selects against the *URA3 CDC9* plasmid. *cdc9*Δ cells can grow on 5-fluoroorotic acid if they have been transformed with a second *CEN TRP1* plasmid containing the wild-type *Chlorella* virus ligase gene driven by a constitutive yeast promoter (Fig. 8). The *K186A*, *K188A*, and *E194A* ligase alleles were unable to complement *cdc9*Δ (Fig. 8). Thus, the *in vivo* lethality of these mutations correlated with their catalytic defects in nick joining *in vitro*. The exceptional case was *D192A*, which sustained growth of *cdc9*Δ on 5-fluoroorotic acid (Fig. 8). Further testing of the growth properties of the *D192A* strain on rich medium (yeast extract/peptone/dextrose agar) revealed a thermosensitive growth defect whereby *D192A* cells grew as well as *WT-ChV* cells at 25 and 30 °C (as gauged by colony size) but only formed pinpoint colonies at 37 °C (not shown). It is possible that the D192A mutant is more active when expressed in yeast at 25–30 °C than when expressed in bacteria at 17 °C, which is how the recombinant ligases were produced for biochemical analysis.

DISCUSSION

The present study highlights the roles of motif V residues Lys^{186}, Lys^{188}, Asp^{192}, and Glu^{194} in the nick joining reaction of *Chlorella* virus DNA ligase. Lys^{186}, Lys^{188}, Asp^{192}, and Glu^{194} are implicated in the first step of the pathway, the reaction of ligase with ATP to form the ligase-AMP intermediate. Lys^{188} is also implicated in step 3, the attack of the 3′OH on DNA-adenylate to form the DNA phosphodiester. Plausible mechanistic interpretations of the mutational effects can be made in light of sequence comparisons and reference to the available crystal structures of DNA ligases and capping enzyme captured

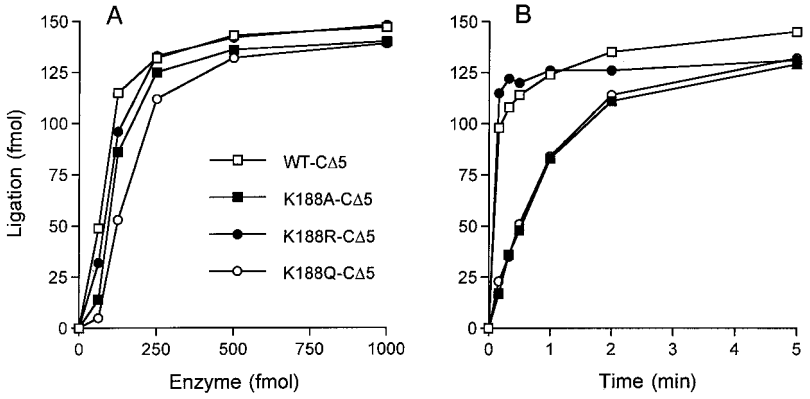

FIG. 7. **Effects of Lys[188] mutations on strand joining at a pre-adenylated nick.** *A*, enzyme titration. The extent of ligation in a 30-min reaction is plotted as a function of input enzyme. *B*, kinetics. Reaction mixtures contained (per 20 μl) 200 fmol of nicked DNA-adenylate substrate and 1 pmol of WT-CΔ5, K188A-CΔ5, K188R-CΔ5, or K188Q-CΔ5. The extent of ligation is plotted as a function of reaction time.

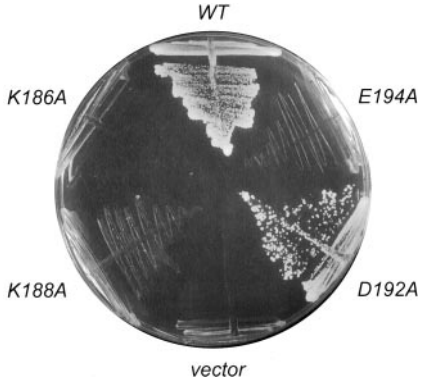

FIG. 8. **Mutational effects on ligase activity *in vivo*.** Yeast strain YBSΔL1 (*cdc9*::*LEU2* p360-*CDC9*) was transformed with *CEN TRP1* plasmids containing WT ChV ligase gene or the indicated mutant alleles (10). Trp^+ isolates were streaked on agar plates containing 0.75 mg/ml 5-fluoroorotic acid. The plates were photographed after incubation for 3 days at 30 °C.

at different steps of the nucleotidyl transfer pathway (2–6).

Motif V residue Lys^{186} is conserved in ATP-dependent DNA ligases and RNA guanylyltransferases but is conspicuously absent from motif V of the NAD^+-dependent bacterial DNA ligases where the corresponding position is occupied by alanine (Fig. 1*A*). Phylogenetic considerations alone would implicate the proximal motif V lysine in a step of the reaction that is shared by ATP-dependent ligases and GTP-dependent capping enzymes but not by the NAD^+-dependent ligases. Given that the ATP and NAD^+ ligase reactions are chemically equivalent subsequent to ligase-AMP formation, it is sensible that elimination of the Lys^{186} side chain did not impact appreciably on the rates of the step 2 plus step 3 reactions under single-turnover conditions. The distinctive common step at which the proximal motif V lysine acts would logically be the reaction with NTP, which entails expulsion of pyrophosphate in the case of ATP ligase and capping enzymes but involves reaction with NAD^+ and expulsion of nicotinamide mononucleotide in the case of bacterial DNA ligases. Indeed the biphasic kinetics of the K186A protein indicated that the reaction of K186A with ATP was rate-limiting under multiple-turnover conditions.

The crystal structure of the *Chlorella* virus ligase-AMP intermediate contains a single sulfate group located on the surface of the ligase adjacent to the phosphate of AMP. The sulfate is believed to mimic the 5′ PO_4 of the nick during step 2 and the γ phosphate of ATP during step 1 (4). The structure shows that Nζ of Lys^{186} makes a bifurcated interaction with a nonbridging phosphate oxygen of the covalently bound adenylate and with the sulfate. Thus, Lys^{186} might interact with the γ phosphate or the α phosphate of ATP during step 1. An instructive point gleaned from the crystal structure of the closed complex of *Chlorella* virus capping enzyme bound to GTP (*i.e.* the ground state immediately prior to step 1 catalysis) is that the equivalent motif I lysine side chain (Lys^{234}) interacts closely with the γ phosphate (at a distance of 2.6 Å from Lys Nζ to a nonbridging oxygen), whereas it does not coordinate the α phosphate (the closest approach being 3.4 Å from Lys^{243} Nζ to the bridging O5′ of the ribose sugar) (2). Guided by this structure, we propose a role for Lys^{186} of *Chlorella* virus DNA ligase in positioning the PP_i leaving group apical to the attacking motif I lysine nucleophile during step 1. This orientation of PP_i is critical for reaction chemistry to proceed through a proposed in-line mechanism (2, 4). There is no γ phosphate in NAD^+ and hence no need for a proximal motif V lysine to interact with this component of the leaving group during the step 1 adenylation reaction of NAD^+-dependent ligases.

Residues Asp^{192} and Glu^{194} of motif V are located within a β strand on the domain 2 side of the interdomain flexion point. The present study implicates both of the acidic side chains in the ligase adenylation step of the pathway. The ligase-AMP crystal structure is construed to reflect the state of the enzyme as it binds to nicked DNA and performs step 2 chemistry. Consequently the protein surface above the adenylate is wide open, and domain 2 has moved away from the active site to make way for DNA. Comparison to the closed structure of the capping enzyme-GMP adduct indicates that the domain movement is achieved by retroflexion of motif V between the component β strands. Asp^{192} and Glu^{194} are not near the adenylate in the open ligase-AMP structure nor do they make instructive contacts with other residues of the ligase (4). Mutational analysis of motif V of *S. cerevisiae* capping enzyme Ceg1 identified an essential aspartate (Asp^{257}) within the distal β strand of motif V (Fig. 1*A*) (17). Wang *et al.* (11) reported that mutation of Asp^{257} to asparagine was lethal, whereas introduction of glutamate restored activity *in vivo*. We suggest that one or both of the essential motif V carboxylates in *Chlorella* virus DNA ligase may play a role similar to that of the essential aspartate of Ceg1. The equivalent motif V aspartate (Asp^{244}) in the crystal structure of the closed conformation of *Chlorella* virus capping enzyme interacts with the β and γ phosphates of GTP, with a lysine side chain in motif VI (RXDK) that contacts the γ phosphate of GTP, and with the arginine of motif VI, which contacts the β phosphate of GTP. The closeness of the Asp^{244} carboxylate oxygens to the nonbridging β and γ phosphate oxygens (2.9 and 3.2 Å) is inconsistent with the expected repulsion between two negatively charged species, which raises the prospect that the carboxylate engages the PP_i leaving group indirectly via water molecules or (more likely) a metal ion coordinated between the β and γ phosphates. We speculate that the motif V carboxylates of the DNA ligase are also interacting with and positioning the PP_i leaving group in step 1, which accounts for the selective effects of the D192A and E194A mutations on ligase adenylation. The two acidic resi-

dues are conserved in motif V of the bacteriophage T7 DNA ligase (Fig. 1*A*), but their function has not been tested via mutagenesis. Other members of the ATP-dependent ligase and capping enzyme families contain at least one carboxylate within the distal segment of motif V. Of note, we found that alanine mutation of the lone glutamate in the distal part of motif V of *E. coli* DNA ligase had no effect on nick joining (12), but, as discussed above, the NAD^+-dependent ligases will interact differently with the nicotinamide mononucleotide leaving group.

A key insight from the present study is that the second of the two conserved motif V lysine residues (Lys^{188}) is specifically important for catalysis of step 3. This is the first instance for an ATP-dependent ligase in which a single mutation elicited a step 3 block with accumulation of DNA-adenylate intermediate. Lys^{188} is conserved in ATP-dependent ligases, capping enzymes, and even NAD^+-dependent DNA ligases (Fig. 1*A*). It is remarkable that an alanine mutation of the solo motif V lysine of *E. coli* DNA ligase had the same effect of arresting step 3 and causing accumulation of very high levels of the DNA-adenylate intermediate during single-turnover nick joining (12). The concordance of the step 3 mutational effects at this lysine in ATP-dependent and NAD^+-dependent ligases underscores how the mechanism of phosphodiester bond formation by the two DNA ligase families is fundamentally similar.

In the *Chlorella* virus ligase-AMP crystal, the Lys^{188} side chain is located on the protein surface with Nζ at a distance of about 5.5 Å from the AMP phosphate and 9–10 Å from the sulfate. Lys^{188} makes no direct contacts with other residues of the ligase. Thus, if Lys^{188} were to promote step 3 via interaction with the reactive 5′ AppDNA end of the nick, a conformational rearrangement of the protein or the AppDNA end (or both) would be required after step 2 catalysis relative to the structure seen for ligase-AMP. An alternative model is that K188A promotes the formation of a phosphodiester via interaction with the 3′ OH DNA strand at the nick, in which case the position of Lys^{188} in the ligase-AMP crystal might be appropriate as it is in the crystal and would thereby provide clues to the orientation of the nicked DNA termini on the protein surface. The latter model invoking interaction of Lys^{188} with the 3′ OH strand is consistent with the finding that the K188A mutant is able to bind to DNA adenylate, insofar as we have shown that the 3′ OH is not required for nick recognition by *Chlorella* virus DNA ligase (14). Ultimately, clarification of the step 3 mechanism and the specific contacts at the reactive termini will depend on crystallization of the ligase bound to the nicked DNA-adenylate ligand. Step 3 arrest mutants such as K188A or K188Q may be of use in trapping the reaction intermediate *in crystallo*.

REFERENCES

1. Shuman, S., and Schwer, B. (1995) *Mol. Microbiol.* **17,** 405–410
2. Håkansson, K., Doherty, A. J., Shuman, S., and Wigley, D. B. (1997) *Cell* **89,** 545–553
3. Subramanya, H. S., Doherty, A. J., Ashford, S. R., and Wigley, D. B. (1996) *Cell* **85,** 607–615
4. Odell, M., Sriskanda, V., Shuman, S., and Nikolov, D. B. (2000) *Mol. Cell* **6,** 1183–1193
5. Singleton, M. R., Håkansson, K., Timson, D. J., and Wigley, D. B. (1999) *Structure* **7,** 35–42
6. Lee, J. Y., Chang, C., Song, H. K., Moon, J., Yang, J., Kim, H. K., Kwon, S. T., and Suh, S. W. (2000) *EMBO J.* **19,** 1119–1129
7. Lehman, I. R. (1974) *Science* **186,** 790–797
8. Shuman, S. (2000) *Prog. Nucleic Acids Res. Mol. Biol.* **66,** 1–40
9. Sriskanda, V., and Shuman, S. (1998) *Nucleic Acids Res.* **26,** 525–531
10. Sriskanda, V., and Shuman, S. (1998) *Nucleic Acids Res.* **26,** 4618–4625
11. Wang, S. P., Deng, L., Ho, C. K., and Shuman, S. (1997) *Proc. Natl. Acad. Sci. U. S. A.* **94,** 9573–9578
12. Sriskanda, V., Schwer, B., Ho, C. K., and Shuman, S. (1999) *Nucleic Acids Res.* **27,** 3953–3963
13. Ho, C. K., Van Etten, J. L., and Shuman, S. (1997) *J. Virol.* **71,** 1931–1937
14. Odell, M., and Shuman, S. (1999) *J. Biol. Chem.* **274,** 14032–14039
15. Sriskanda, V., and Shuman, S. (2002) *Nucleic Acids Res.*, in press
16. Sekiguchi, J., and Shuman, S. (1997) *J. Virol.* **71,** 9679–9684
17. Shuman, S., Liu, Y., and Schwer, B. (1994) *Proc. Natl. Acad. Sci. U. S. A.* **91,** 12046–12050